IIETA International Information and Engineering Technology Association
Advancing the World of Information and Engineering

Journal Européen des Systèmes Automatisés
Vol. 57, No. 5, October, 2024, pp. 1249-1257
Journal homepage: http://iieta.org/journals/jesa

Advanced Diagnosis of Air Gap Eccentricity in Three-Phase Induction Motor Using DWT Decomposition and AI Techniques

Moutaz Bellah Bentrad[1*], Adel Ghoggal[1], Tahar Bahi[2]

[1] Electrical Engineering Laboratory of Biskra (LGEB), Mohamed Khider University, Biskra 07000, Algeria
[2] LASA Laboratory, Badji Mokhtar University, Annaba 23000, Algeria

Corresponding Author Email: moutazbellah.bentrad@univ-biskra.dz

https://doi.org/10.18280/jesa.570501

Received: 16 July 2024
Revised: 29 September 2024
Accepted: 10 October 2024
Available online: 28 October 2024

Keywords:
induction machine, stator current, air gap eccentricity, DWT, machine learning

ABSTRACT

Early fault detection for the induction machine became a necessity to prevent the escalation of failures to severe levels, thereby avoiding unscheduled downtimes. Among the various failure modes in electrical machines, rotor-related faults, such as air gap eccentricity, require particular attention and to detect this type of defects model-based methods are extensively used in this field. However, because of the intricacies of the diagnosed model and the time-consuming investigations it renders the diagnosis process more laborious and less efficient. This article focuses on applying a non-model based approach that relies in general on feature extraction using discrete wavelet transform decomposition analysis of stator current signal for various stages of air gap eccentricity and under multiple operating conditions and as a first step of the conducted work, through performing an in-depth energy distribution analysis through all of the decomposed signal levels to extract the best sub-signal level that holds the most relevant information about the machine's condition alongside to RMS values of the signal. The second part of the research focuses on employing the extracted features as input data used for training a multi-layer perceptron algorithm such as support vector machine and decision trees. Our endeavor is to choose the most accurate algorithm for the multiclass classification.

1. INTRODUCTION

Electrical machines, like any mechanism, are prone to undesirable sudden breakdowns that may hinder the industrial process from functioning properly. This could lead to critical economic losses and, in some cases, may endanger the operating personnel due to hazardous threats that the breakdowns may cause.

The importance of three-phase induction motors (IM) across various industries is due to their ability to generate high motive power, their durability, and their low maintenance costs. These motors serve as the primary mover in about 90% of industrial equipment worldwide, highlighting their crucial role in industrial operations [1].

Induction machine faults have been diagnosed using various frequency analysis methods, including fast Fourier transform (FFT), power spectrum estimation, and envelope spectrum analysis [2]. The disadvantage of this technique is based on the fact that it requires that the signal being processed is stationary and linear and that the rotational speed has transient mode, which represents a limitation by this technique. Therefore, to mitigate this obstacle a Time-Frequency analysis is performed such as Short Fast Fourier Transform (STFT) [3], the premise of this technique is based on the FFT method with applying a sliding window to enhance the frequency resolution. However, the limitation of this method is the fixed size of the window which is not practical with the transient nature of the signal. Another method is being applied for this regard, Wigner-Ville distribution (WVD) [4] which delivers better frequency resolution under the same conditions, another drawback of this approach is the generation of undesirable large frequencies. Empirical mode decomposition (EMD) [5-7] on the other hand, is a self-adaptive approach, which produce a series of intrinsic mode functions (IMFs) and with the help of the Hilbert Transform (HT) [8], it can estimate instantaneous frequencies, but its limitation resides on the generation of undesirable negative frequencies. Wavelet Transform (WT) delivers an enhanced frequency resolution results thanks to its local frequency-time domain properties [9].

This work's focus orbits around the combination of signal processing through Discrete Wavelet Transform (DWT) decomposition of the stator current signal and an Artificial Intelligence (AI) driven model that utilizes the denoised data signal and through a meticulous study of the decomposed levels, the most suitable frequency detail band level was chosen to be used for feature extraction by using both of energy distribution analysis and RMS values, both of these factors will be introduced as inputs for machine learning algorithms such as Support Vector Machine (SVM) and Decision Trees (DT).

1.1 Related works

Widagdo et al. [10] mentioned that failures due to air gap

eccentricity are predicted by decomposing the leakage flux spectrum waveform using discrete wavelet transform. This method was tested using the leakage flux data from a 1.5 Kw induction motor. Experimental results validated the effectiveness of this approach in detecting eccentricity failures.

Nikhil et al. [11] used various indices to detect eccentricity are introduced, along with their boundary conditions and potential areas for future research. Finally, the merits and demerits of each index are discussed, and a comparison is made between them.

Rouaibia et al. [12] introduced two methods for diagnosing and detecting eccentricity faults, as well as evaluating their severity, by monitoring stator current signals. The approaches use the Park vector method and DWT to differentiate between healthy and faulty machine conditions. The simulation results obtained through these techniques enable the detection and diagnosis of eccentricity faults and their severity.

Laala et al. [13] presented a contribution in the classification of a vibration signal for bearing fault, where wavelet packet decomposition (WPD) and multi-layer perceptron (MLP) were combined. At first, the most suitable component to bearing defect was used as a fault indicator. Then, feature extraction was used for the classification by MLP algorithm.

2. AIR GAP ECCENTRICITY MODEL

The data collected is from three phase squirrel cage model, Table 1 illustrates the parameters of the machine.

Table 1. Induction machine parameters

Parameter	Identification
Machine type	3-phase squirrel cage with inclined bar
Number of bars	40
Frequency	50 Hz
Rated Voltage	415 V
Winding number	28
Air gap radius	82 mm
Air gap thickness	0.8 mm
Rotor length	0.11 m
Rotor leakage inductance	6.1 mH
Rotoric bar resistance	31×10^{-6} Ω
Rotoric bar leakage inductance	0.095×10^{-6} H
Stator phase resistance	1.75 Ω
Short circuit ring resistance	2.2×10^{-6} Ω
Short circuit ring segment leakage inductance	0.018×10^{-6} H
Permeability	12.56×10^{-7} H/m

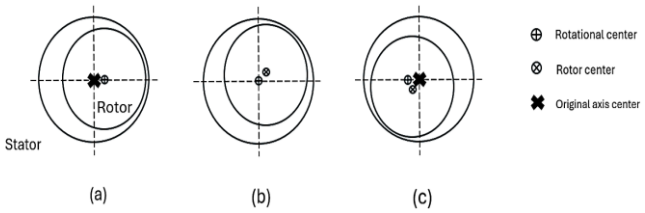

Figure 1. Eccentricity types: a-static, b-dynamic, c-mixed

Air gap eccentricity in a three-phase induction motor occurs when the rotor (the rotating part) is not correctly aligned with the stator magnet (the stationary part). This misalignment causes the distance between the rotor and stator surfaces (the air gap) to be uneven around the rotor's circumference [14]. Among the most frequent mechanical faults that can affect induction motors, one that stands out extensively is eccentricity, a fault that can manifest in static, dynamic or the combination between both in mixed eccentricity [15-17]. Figure 1 clearly shows the various types of eccentricity [18].

Figure 2 illustrates air gap eccentricity impact on the current signal, it's notable that at early stage there's no visible change in the wave form of the current, only in extreme stage.

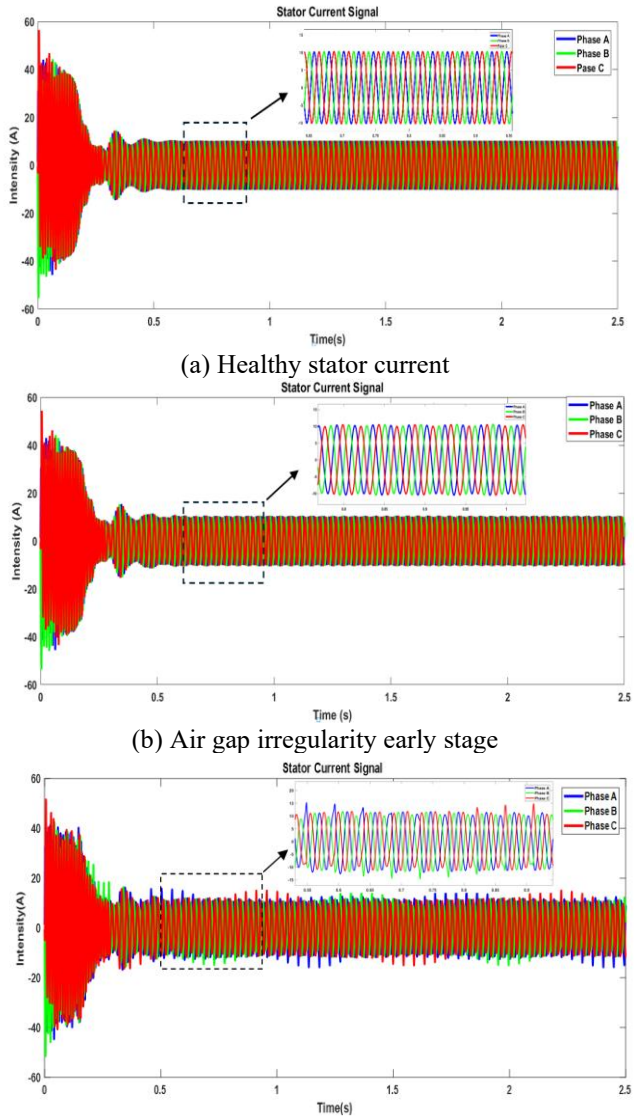

Figure 2. Eccentricity influence on stator current

Air gap irregularity is a common defect that happens frequently and it can manifest even in newly fabricated machines since the margin between the stator and the rotor circuit is too thin which is called the air gap. Therefore, the chosen profile for air gap eccentricity for this research would be set to 10% deemed tolerable, 20% noticeable with a degree of a precaution when dealing with the defected machine, 30% is an alarming rate and requires an immediate intervention to prevent from condition deterioration which could lead to other undesirable defects (deterioration of insolation condition, short-circuit, rising temperature...etc.).

Despite the fact that even in newly manufactured machines a 10% of air gap irregularity exists, and its up to the manufacturer to reduce this level to its minimum value [19];

researchers chose 20% for static and 38.46% for dynamic eccentricity levels as prominent thresholds since they can be suitable index for the diagnosis, the more eccentricity level increases the more the harmonic component increases also [20].

2.1 Frequency domain analysis

Stator current frequency analysis equation in induction machines can be determined as follows [21]:

$$f_{ec} = f_1\left[\left(k_1 R \pm \underline{n}_d\right)(1-s)/p \pm v\right] \quad (1)$$

As was previously mentioned, FFT delivers a strong analysis in the frequency domain. However, it struggles when dealing with a non-stationary signal, which is a huge drawback of this technique that causes spectral leakage of the hidden frequencies that hold important information about the condition of the machine, which would be afterwards critical for decision making.

Linear spectral analysis has been performed on the current signal for both healthy and faulty machines to extract frequency information related to the defect and it has been shown in Figure 3.

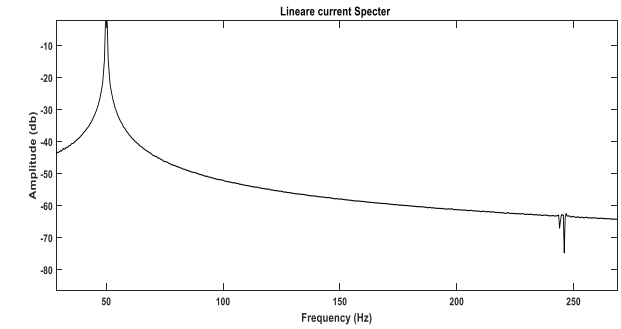

(a) Linear specter of healthy stator current

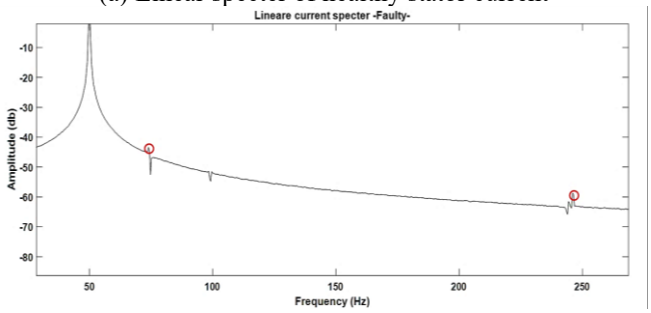

(b) Linear specter of faulty stator current

Figure 3. Linear spectral analysis

3. DISCRETE WAVELET TRANSFORM

To mitigate the limitation of FFT technique when dealing with non-stationary signal, WT delivers a robust time-frequency domain analysis for both stationary and non-stationary signals, and among its tools DWT is the most efficient technique in terms of computational capabilities which gives more accuracy when dealing with non-stationary signal and especially at low frequency [22, 23]:

$$DWT(J,k) = \frac{1}{\sqrt{2^J}}\int_{-\infty}^{+\infty} x(t)\psi^*\left(\frac{t-k\cdot 2^J}{2^J}\right)\mathrm{d}t = 2^{\frac{-J}{2}}\psi(2^{-J}\cdot t - k) \quad (2)$$

DWT relies on the decomposition of the raw signal back to its constituent point (scales), which give us an information about the frequency band at a particular time frame.

DWT is conducted through a sequential operation using a high-pass filters H (details) and through a series of low-pass filters L (approximations).

Figure 4 shows the decomposition process of DWT starting from raw signal until getting subsignals.

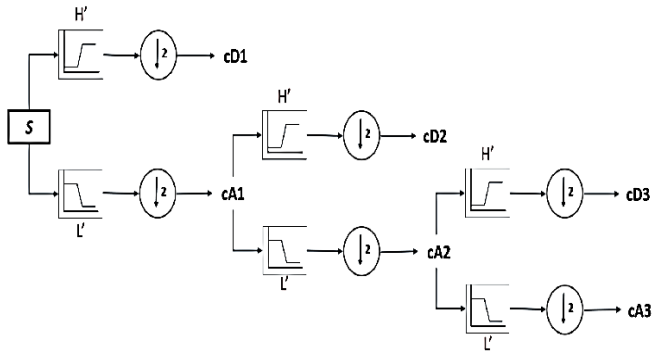

Figure 4. DWT decomposition process

Raw signal *x(t)* is divided into two ports, the first one contains the high frequency band, and the second one low frequency band, both of them are combined for the decomposition and the reconstruction of the original signal [24, 25].

The low frequency part called approximations (A_j) contains the low-frequency information of the original signal belong to [0, *fs*·2–(*j*+1)]. The high-frequency part called detail (D_j) contain high frequency information included in the interval [*fs*·2–(*j*+1), *fs*·2–*j*]. Practically, the DWT decomposition at level N of signal *x(t),* giving rise to one approximation coefficient vector AN and N detail coefficient vectors D_j are expressed by [26, 27]:

$$x(t) = A_N(t) + \sum_{j=1}^{N} D_j(t) \quad (3)$$

It can be shown that the approximation and detail coefficients can be recursively calculated by:

$$A_{j,k} = \sqrt{2}\sum_{-\infty}^{+\infty} L[n]A_{j-1,2k+n} \quad (4)$$

$$D_{j,k} = \sqrt{2}\sum_{-\infty}^{+\infty} H[n]A_{j-1,2k+n} \quad (5)$$

Before getting into the mother wavelet function selection, it is mandatory to choose the number of decomposition levels that are suitable to cover all of the details and approximations frequency range, which can be determined by the following equation:

$$\frac{f_s}{2^{N+1}} \leq f_e \quad (6)$$

where, f_e which is the fundamental frequency, and f_s is the sampling frequency set to f_s=10KHz.

3.1 Time-frequency domain analysis

The first step of the research is to perform a full decomposition of the stator raw current signal, and to achieve this 1-D DWT decomposition was used up to 12 levels to cover all the ranges of frequency bands of both approximations and details by using debauchees -24 as the mother wavelet function and the sampling frequency was set to 10KHz. Full decomposition results for both healthy and air gap irregularity current signals were collected to be compared later on (Figure 5).

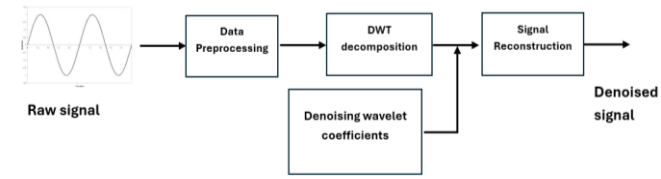

Figure 5. DWT signal decomposition and reconstruction

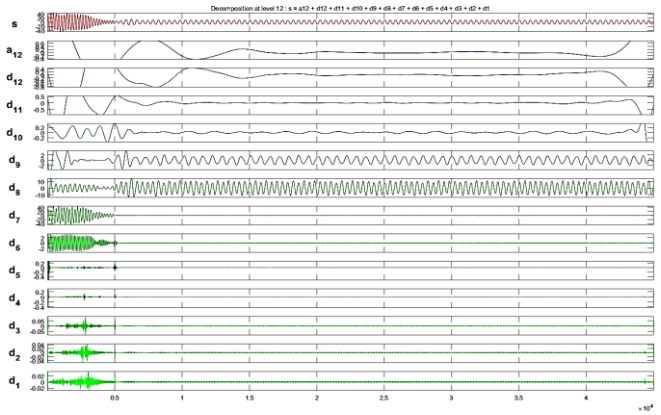

(a) Decomposition levels of a healthy signal

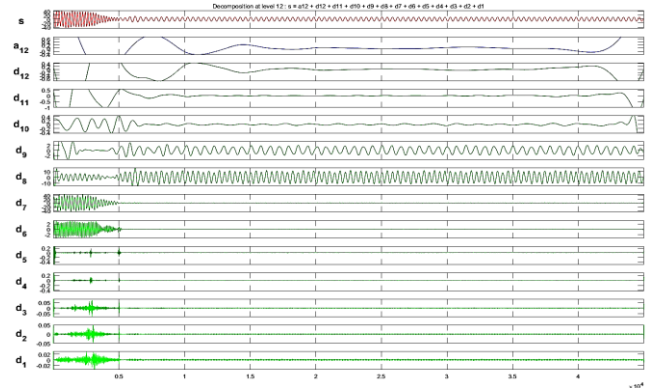

(b) Decomposition levels of a faulty signal

Figure 6. Full decomposition of stator current

Till the present day, there's no specific rule that dectates the choice of a specific mother wavelet. However, through various deep studies it was noticed that Debauchees mother wavelet povides more stability and a robust reconstruction of the original signal with maintaining information since it locates less in time with less oscillation due to its dilation nature, which makes it practical for the diagnosis of induction machine [28]. Figure 6 shows the complete decompostion usnig DWT of raw current signal for healthy and faulty machines.

After analyzing the obtained results of the full decomposition for both approximation and detail frequencies in healthy and faulty condition, we can notice that air gap irregularity manifests some changes in high frequency (detail frequency) band [1000-5500Hz] and they're more visible in levels 4, 5 and 6, which can deliver a promising comparison opportunity, further results are discussed thoroughly in the next section.

Three decomposition levels were selected since they show promising characteristic comparison and contain inherent frequency that characterize air gap defect which are levels 4, 5 and 6th level of detail decomposition illustrated in Figure 7.

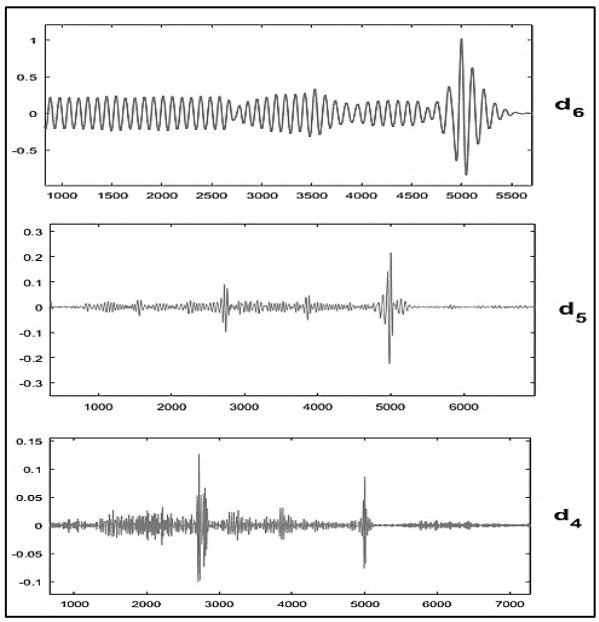

(a) Healthy detail frequency levels

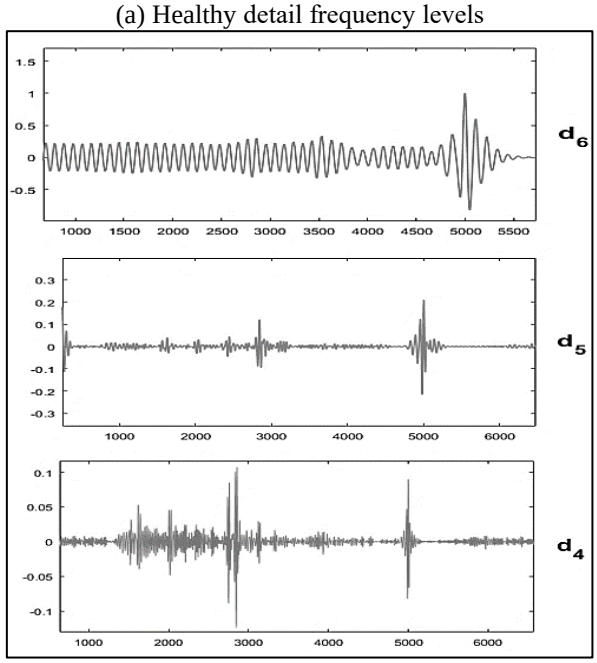

(b) Faulty detail frequency levels

Figure 7. Detail levels 4, 5 and 6

4. ENERGY DISTRIBUTION ANALYSIS

4.1 Wavelet energy

The consumed energy at each level of decomposition is calculated, to identify and validate the frequency bands containing the defect frequency for both faulty and healthy

cases under different load conditions. For this purpose, the energy linked to each D_j detail signal of the torque signal is expressed as follow:

$$E_j = \sum_{k=1}^{n} D_{j,k}^2(n) \quad (7)$$

where, j is the specific number of the levels of decomposition, $D_{j,k}$ is the magnitude related to the coefficient of the decomposed level j, n is the DWT decomposition time.

An energy distribution analysis was performed in order to determine the most suitable and pertinent detail levels that dissipate more energy under various operating conditions and for various severity degree of the defect for each type of air gap eccentricity, the results are shown in Figure 8.

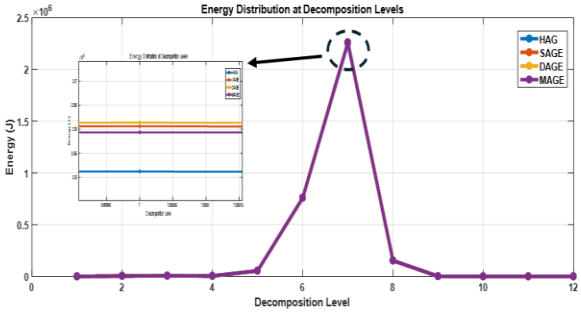

(a) Energy distribution analysis of the decomposition levels at early stage of air gap irregularity weak load

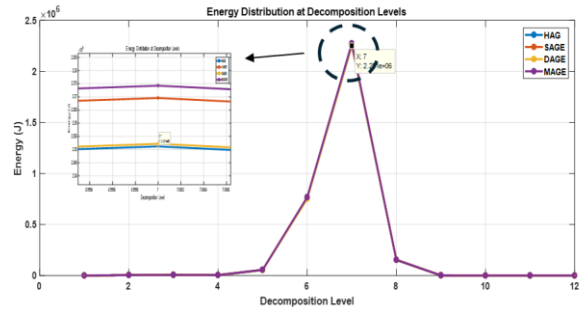

(b) Energy distribution analysis of the decomposition levels at 30% air gap irregularity weak load

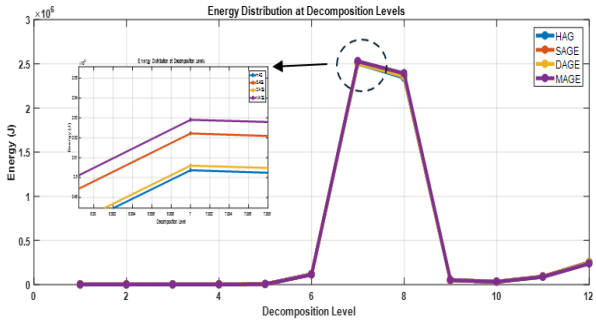

(c) Energy distribution analysis of the decomposition levels at 30% air gap irregularity medium load

Figure 8. Energy distribution analysis under various conditions for air gap types

It became evident that the most pertinent results for energy distribution reside in levels 6, 7 and 8 with a prominent advantage for level 7, that exhibits the peak of energy dissipation for all of the operating conditions and under various fault types and severity degrees.

Detailed results of dissipated energy levels are shown in Table 2.

Table 2. Dissipated energy through decomposition levels

Machine Condition	Decomposition Level	Dissipated Energy (J)
HAG	D6	1.173×10^5
	D7	2.504×10^6
	D8	2.344×10^6
SAGE	D6	1.164×10^5
	D7	2.522×10^6
	D8	2.363×10^6
DAGE	D6	1.155×10^5
	D7	2.206×10^6
	D8	2.359×10^6
MAGE	D6	1.126×10^5
	D7	2.529×10^6
	D8	2.392×10^6

5. ARTIFICIAL INTELLIGENCE MODEL

5.1 Support vector machine (SVM)

SVM branches out from machine learning models under supervised learning algorithms by performing a linear classification for a multiclass dataset. It provides great generalization abilities even when dealing with a small number of dataset samples [29]. Its architecture is shown in the Figure 9 [30], the margin in this structure is the distance between the decision boundaries and the support vectors, while the latter contains the group of data samples that are approximate to decision boundary which represents a hyperplane of the linear classification [31].

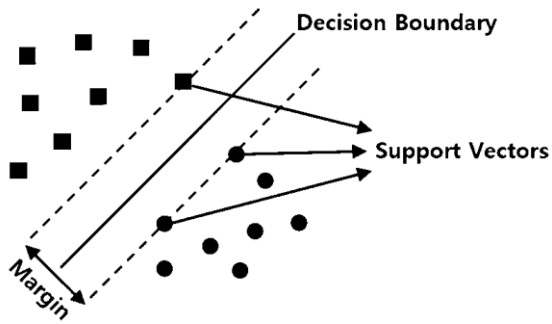

Figure 9. SVM basic architecture

The decision boundary is determined by the following equation:

$$\mathrm{d(x)} = \mathrm{w}x_i + \mathrm{b} \quad (8)$$

where, w is the weight vector, x_i is the input data and b is the bias.

The distance of the margin can be obtained as follows:

$$\text{margin} = \frac{2}{\| w \|} + \mathrm{C}\sum_{i=1}^{n} \xi_i \quad (9)$$

In case of misclassification where the data can't be linearly classified ξ is the variable slack that can adjust the rate of misclassification, C is a parameter defined by the user, the

higher this parameter's value, the lower the degree of misclassification.

5.2 Decision trees

Decision Trees (DT) is one of the strongest classification algorithms and used in many fields [32], it effectively unites a series of basic test, the construction of conceptual rules are easier in comparison with the numerical weights which are used in neural networks of connections between nodes [33, 34]. Each one of the trees compose the branches and the nodes, those nodes each one of them represents a feature that would be classified, the value taken by the node is defined by each subset. Figure 10 shows how decision trees algorithm works starting with the root node responsible for dividing into decision nodes

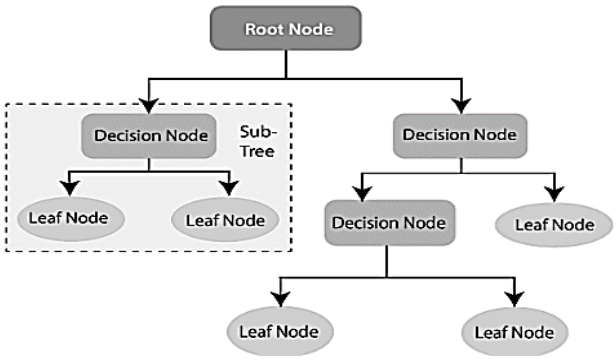

Figure 10. DT process

6. PROPOSED METHODOLOGY

The proposed method is based on two steps, in the first section of the paper, a signal processing was employed using DWT full decomposition, in order to denoise our raw current signal for the purpose of extracting the most suitable feature from the obtained signal, then an energy distribution analysis was conducted in order to choose the best frequency band sensitive to the variations of current signal for both healthy and faulty machines, root mean square (RMS) was backed as a fault indicator to reinforce the learning process in the upcoming section. Later, an AI-based diagnosis was performed using machine learning algorithms in hope to classify the chosen dataset into 3 classes: fault type, fault localization and severity degree as shown in Figure 11.

6.1 Machine learning application

In this section, two machine learning algorithms were employed for the diagnosis of air gap eccentricity, the first algorithm is SVM, after training our model using energy levels and RMS values as inputs the results of testing the model's precision is shown in the confusion matrix (Figure 12).

SVM model exhibited some satisfying results when classifying early stage degrees for both static and dynamic air gap eccentricity which served the purpose of monitoring of this defect with an overall accuracy above 70% and also the detection of the fault itself by successfully distinguishing healthy samples from the faulty ones with an accuracy of 79%.

The chosen architecture for SVM model is shown in the following Table 3. The evaluation of SVM model results are shown in Table 4.

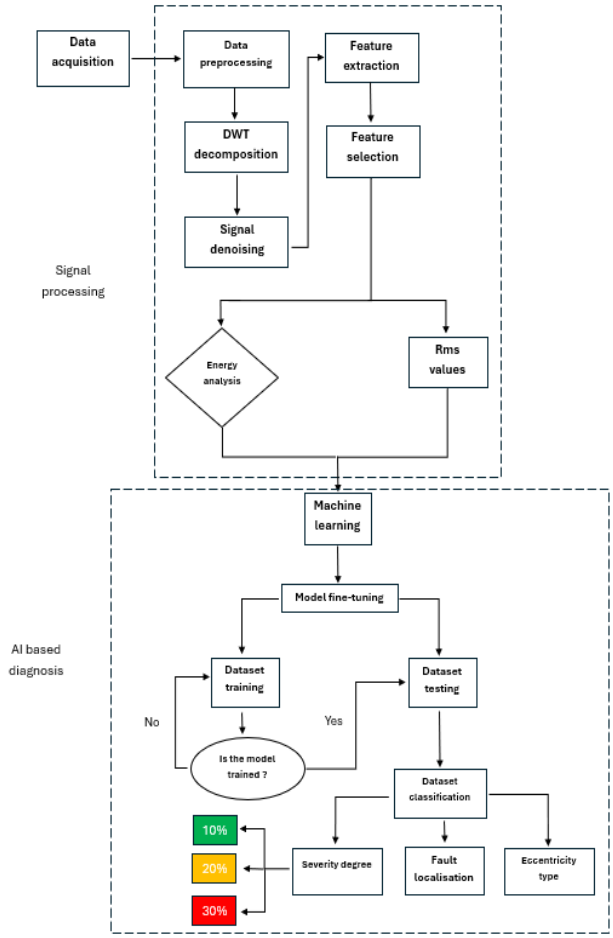

Figure 11. Diagnosis process flowchart

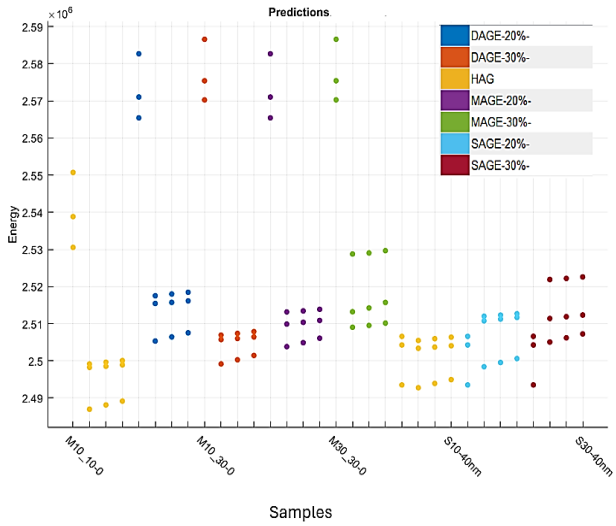

Figure 12. Data scatter plot based on severity degree and dissipated energy levels

Table 3. SVM chosen architecture settings

Classifier	Parameter	Chosen Setting
SVM	Kernel Function	Linear kernel
	Standardization	Input features are standardized
	Box Constraint	1
	Kernel Scale	Not used
	Multiclass Scheme	One-vs-one

Table 4. SVM evaluation results

Condition	Precision	Recall	F1score
DAGE-20%-	100%	75%	85%
DAGE-30%-	80%	66%	72%
HAG	84%	87.5%	85.7%
MAGE-20%-	100%	75%	85.7%
MAGE-30%-	47%	66%	55%
SAGE-20%-	69%	75%	72%
SAGE-30%-	53%	58%	56%

The second machine learning algorithm chosen is DT algorithm, which delivered outstanding results in comparison to SVM model by successfully classifying the defected samples and the healthy ones and each type of the defect alongside its severity degree. The chosen architecture for DT model is shown in Table 5.

Table 5. DT chosen architecture settings

Classifier	Parameter	Chosen Setting
DT	Splitting Criterion	Gini's diversity index
	Max Splits	100
	Minimum Leaf Size	1
	Maximum Tree Depth	No strict cap
	Pruning	Post-pruning
	Surrogate Splits	Not used

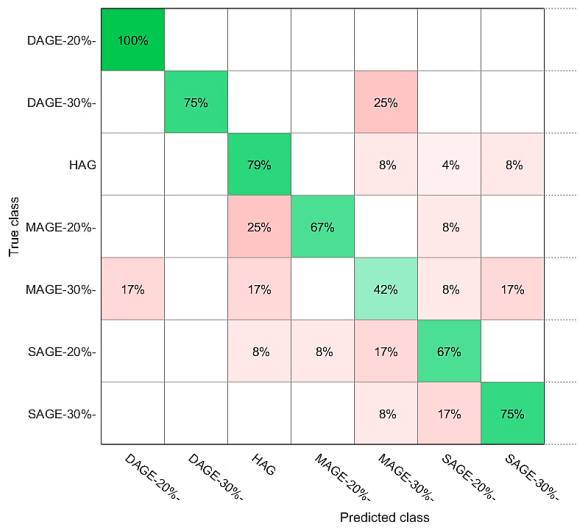

Figure 13. Confusion matrix results using SVM

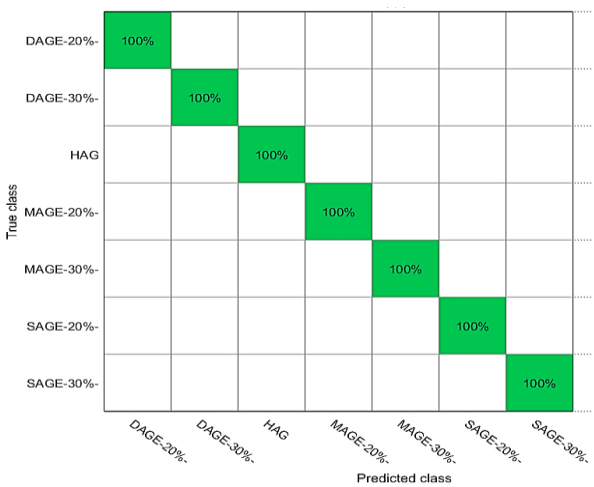

Figure 14. Confusion matrix results using DT

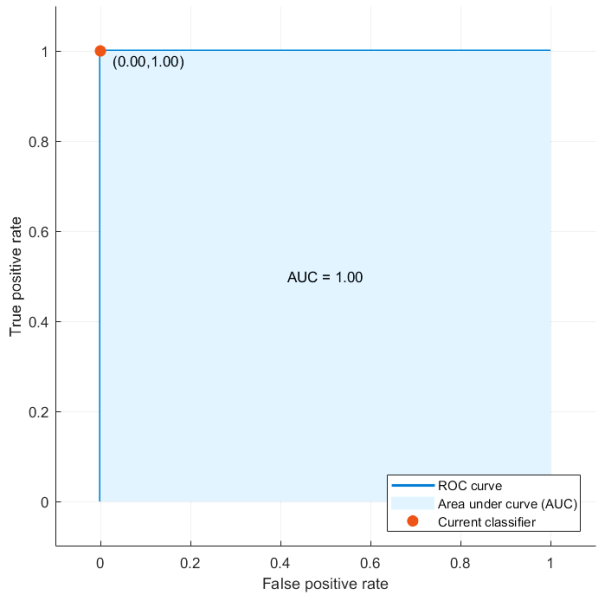

Figure 15. ROC curve plot

The results of classification are shown in the confusion matrix (Figure 13).

Confusion matrix results are illustrated in Figure 14, that shows outstanding performance results and classification capabilities.

DT model achieved 1.00 results at various threshold settings, which indicates that the model has a strong distinguishing capacity between the chosen classes. As was previously illustrated in Figure 15.

7. CONCLUSIONS

After applying the proposed methodology, it becomes evident that using DWT decomposition for the purpose of employing energy dissipation levels and RMS values as fault indicators combined with machine learning, proved reliable for the classification of air gap eccentricity and can serve quite effectively the purpose of monitoring task for this type of defects in induction machine.

The task for choosing the best classifier for the detection of air gap irregularity went through training various models and the best models in terms of accuracy of detection were SVM with an overall 70% accuracy and DT classifier with 100% accuracy.

The main challenge lies in providing more complex data in terms of harmonics and noise in the signal which would render the detection more challenging and would require introducing other models with more specific settings for the hyperparameters. Therefore, the upcoming work will focus on using more features for fault classification and introducing more severity degrees in hope of achieving a global diagnosis process with maintaining a strong monitoring capability.

REFERENCES

[1] Okwuosa, C.N., Akpudo, U.E., Hur, J.W. (2022). A cost-efficient MCSA-based fault diagnostic framework for SCIM at low-load conditions. Algorithms, 15(6): 212. https://doi.org/10.3390/a15060212

[2] Li, H., Zhang, Y., Zheng, H. (2010). Bearing fault

detection and diagnosis based on order tracking and Teager-Huang transform. Journal of Mechanical Science and Technology, 24(3): 811-822. https://doi.org/10.1007/s12206-009-1211-9

[3] Gimm, H.I., Cha, K.U., Cho, C.K. (2012). Characterizations of gun barrel vibrations of during firing based on shock response analysis and short-time Fourier transform. Journal of Mechanical Science and Technology, 26: 1463-1470. https://doi.org/10.1007/s12206-012-0335-5

[4] Liu, L., Luo, M., Lai, L. (2018). Instantaneous frequency estimation based on the Wigner-ville distribution associated with linear canonical transform (WDL). Chinese Journal of Electronics, 27(1): 123-127. https://doi.org/10.1049/cje.2017.07.009

[5] Zhang, X., Zhou, J. (2013). Multi-fault diagnosis for rolling element bearings based on ensemble empirical mode decomposition and optimized support vector machines. Mechanical Systems and Signal Processing, 41(1-2): 127-140. https://doi.org/10.1016/j.ymssp.2013.07.006

[6] Chen, K., Zhou, X.C., Fang, J.Q., Zheng, P.F., Wang, J. (2017). Fault feature extraction and diagnosis of gearbox based on EEMD and deep briefs network. International Journal of Rotating Machinery, 2017(1): 9602650. https://doi.org/10.1155/2017/9602650

[7] Zhao, H., Sun, M., Deng, W., Yang, X. (2016). A new feature extraction method based on EEMD and multi-scale fuzzy entropy for motor bearing. Entropy, 19(1): 14. https://doi.org/10.3390/e19010014

[8] Soualhi, A., Medjaher, K., Zerhouni, N. (2014). Bearing health monitoring based on Hilbert–Huang transform, support vector machine, and regression. IEEE Transactions on Instrumentation and Measurement, 64(1): 52-62. https://doi.org/10.1109/TIM.2014.2330494

[9] Hu, Q., Qin, A., Zhang, Q., He, J., Sun, G. (2018). Fault diagnosis based on weighted extreme learning machine with wavelet packet decomposition and KPCA. IEEE Sensors Journal, 18(20): 8472-8483. https://doi.org/10.1109/JSEN.2018.2866708

[10] Widagdo, R., Hartayu, R., Hariadi, B. (2023). Discrete wavelet transform applied to 3-phase induction motor for air gap eccentricity fault diagnosis. Journal of Electrical Engineering, Mechatronic and Computer Science, 6(2): 111-121. https://doi.org/10.26905/jeemecs.v6i2.10707

[11] Nikhil, Mathew, L., Sharma, A. (2018). Various indices for diagnosis of air-gap eccentricity fault in induction motor—A review. IOP Conference Series: Materials Science and Engineering, 331: 012032. https://doi.org/10.1088/1757-899X/331/1/012032

[12] Rouaibia, R., Arbaoui, F., Bahi, T. (2017). Fault eccentricity diagnosis in variable speed induction motor drive using DWT. Advances in Modelling and Analysis C, 72(3): 181-202. https://doi.org/10.18280/ama_c.720301

[13] Laala, W., Guedidi, A., Guettaf, A. (2023). Bearing faults classification based on wavelet transform and artificial neural network. International Journal of System Assurance Engineering and Management, 14: 37-44. https://doi.org/10.1007/s13198-020-01039-x

[14] Husnah, N., Asfani, D.A., Negara, I.M.Y. (2023). Fault detection experiment of unbalanced voltage and air gap eccentricity on induction motor using a flux sensor. Journal on Advanced Research in Electrical Engineering, 7(1): 20-27. https://doi.org/10.26905/jeemecs.v6i2.10707

[15] Corral-Hernandez, J.A., Antonino-Daviu, J.A. (2018). Thorough validation of a rotor fault diagnosis methodology in laboratory and field soft-started induction motors. Chinese Journal of Electrical Engineering, 4(3): 66-72. https://doi.org/10.23919/CJEE.2018.8471291

[16] Faiz, J., Moosavi, S.M.M. (2017). Detection of mixed eccentricity fault in doubly-fed induction generator based on reactive power spectrum. IET Electric Power Applications, 11(6): 1076-1084. https://doi.org/10.1049/iet-epa.2016.0449

[17] Yassa, N., Rachek, M., Houassine, H. (2019). Motor current signature analysis for the air gap eccentricity detection in the squirrel cage induction machines. Energy Procedia, 162: 251-262. https://doi.org/10.1016/j.egypro.2019.04.027

[18] Samaga, B.R., Vittal, K.P. (2011). Air gap mixed eccentricity severity detection in an induction motor. In 2011 IEEE Recent Advances in Intelligent Computational Systems, pp. 115-119. https://doi.org/10.1109/RAICS.2011.6069284

[19] Faiz, J., Ebrahimi, B.M., Akin, B., Toliyat, H.A. (2007). Finite-element transient analysis of induction motors under mixed eccentricity fault. IEEE Transactions on Magnetics, 44(1): 66-74. https://doi.org/10.1109/TMAG.2007.908479

[20] Roczek, K., Rogala, T. (2019). Induction motor diagnosis with use of electric parameters. Diagnostyka, 20(4): 65-74. https://doi.org/10.29354/diag/113000

[21] Kim, M.C., Lee, J.H., Wang, D.H., Lee, I.S. (2023). Induction motor fault diagnosis using support vector machine, neural networks, and boosting methods. Sensors, 23(5): 2585. https://doi.org/10.3390/s23052585

[22] Hussein, A.M., Obed, A.A., Zubo, R.H., Al-Yasir, Y.I., Saleh, A.L., Fadhel, H., Sheikh-Akbari, A., Mokryani, G., Abd-Alhameed, R.A. (2022). Detection and diagnosis of stator and rotor electrical faults for three-phase induction motor via wavelet energy approach. Electronics, 11(8): 1253. https://doi.org/10.3390/electronics11081253

[23] Garcia-Calva, T.A., Morinigo-Sotelo, D., Fernandez-Cavero, V., Garcia-Perez, A., Romero-Troncoso, R.D.J. (2021). Early detection of broken rotor bars in inverter-fed induction motors using speed analysis of startup transients. Energies, 14(5): 1469. https://doi.org/10.3390/en14051469

[24] Bessam, B., Menacer, A., Boumehraz, M., Cherif, H. (2017). Wavelet transform and neural network techniques for inter-turn short circuit diagnosis and location in induction motor. International Journal of System Assurance Engineering and Management, 8: 478-488. https://doi.org/10.1007/s13198-015-0400-4

[25] Almounajjed, A., Sahoo, A.K., Kumar, M.K. (2021). Diagnosis of stator fault severity in induction motor based on discrete wavelet analysis. Measurement, 182: 109780. https://doi.org/10.1016/j.measurement.2021.109780

[26] Bengharbi, A.A., Laribi, S., Allaoui, T., Mimouni, A. (2022). Photovoltaic system faults diagnosis using discrete wavelet transform based artificial neural networks. Electrical Engineering & Electromechanics, (6): 42-47. https://doi.org/10.20998/2074-

272X.2022.6.07
[27] Akkouchi, K., Rahmani, L., Lebied, R. (2021). New application of artificial neural network-based direct power control for permanent magnet synchronous generator. Electrical Engineering & Electromechanics, (6): 18-24. https://doi.org/10.20998/2074-272X.2021.6.03
[28] Khadim, S. (2016). Early, diagnosis of airgap eccentricity fault in the inverter driven induction motor drives by wavelet transform. Journal of Electrical Engineering, 16: 94. https://doi.org/10.1016/j.pisc.2016.04.014
[29] Shen, L., Chen, S. (2010). A kind of SVM fast training method based on samples segmentation learning. In 2010 4th International Conference on Distance Learning and Education, pp. 6-9. https://doi.org/10.1109/ICDLE.2010.5606051
[30] Jha, R.K., Swami, P.D. (2021). Fault diagnosis and severity analysis of rolling bearings using vibration image texture enhancement and multiclass support vector machines. Applied Acoustics, 182: 108243. https://doi.org/10.1016/j.apacoust.2021.108243
[31] Kankar, P.K., Sharma, S.C., Harsha, S.P. (2011). Fault diagnosis of ball bearings using machine learning methods. Expert Systems with Applications, 38(3): 1876-1886. https://doi.org/10.1016/j.eswa.2010.07.119
[32] Stein, G., Chen, B., Wu, A.S., Hua, K.A. (2005). Decision tree classifier for network intrusion detection with GA-based feature selection. In Proceedings of the 43rd annual Southeast Regional Conference, pp. 136-141. https://doi.org/10.1145/1167253.1167288
[33] Barros, R.C., Basgalupp, M.P., De Carvalho, A.C., Freitas, A.A. (2011). A survey of evolutionary algorithms for decision-tree induction. IEEE Transactions on Systems, Man, and Cybernetics, Part C (Applications and Reviews), 42(3): 291-312. https://doi.org/10.1109/TSMCC.2011.2157494
[34] Gupta, G. (2014). A self explanatory review of decision tree classifiers. In International Conference on Recent Advances and Innovations in Engineering (ICRAIE-2014), pp. 1-7. https://doi.org/10.1109/ICRAIE.2014.6909245

NOMENCLATURE

f_1	Frequency supply, Hz
f_{eq}	Eccentricity frequency, Hz
f_e	Fundamental frequency, Hz
f_s	Sampling frequency, Hz
K_1	Any integer
R	Number of rotor slots
P	Number of pairs of poles
n_d	Eccentricity order
s	Slip
v	Order of stator time harmonics

Greek symbols

ψ	Mother wavelet
ξ	Slack variable

Subscripts

AI	Artificial intelligence
FFT	Fast Fourier transform
DAGE	Dynamic air gap eccentricity
DT	Decision trees
DWT	Discrete wavelet transform
HAG	Healthy air gap
HT	Hilbert transform
MAGE	Mixed air gap eccentricity
MLP	Multi layer perceptron
RMS	Root mean square
SAGE	Static air gap eccentricity
STFT	Short fast Fourier transform
SVM	Support vector machine
WPD	Wavelet packet decomposition
WT	Wavelet transform